
Uncovering Neural Encoding Variability with Infinite Gaussian Process Factor Analysis

Anonymous Author(s)

Affiliation

Address

email

Abstract

1 Gaussian Process Factor Analysis (GPFA) is a powerful factor analysis model for
2 extracting low-dimensional latent processes underlying population neural activities.
3 However, one limitation of standard GPFA models is that the number of latent
4 factors needs to be pre-specified or selected through heuristic-based processes. We
5 propose the infinite GPFA model, a fully Bayesian non-parametric extension of the
6 classical GPFA model by incorporating an Indian Buffet Process (IBP) prior over
7 the factor loading process, such that it is possible to infer the potentially infinite set
8 of likely latent factors active at each time points, in a probabilistically principled
9 manner. Learning and inference in the infinite GPFA model is performed through
10 variational expectation-maximisation, and we additionally propose a scalable exten-
11 sion based on sparse variational Gaussian Process methods. We empirically
12 demonstrate that the infinite GPFA model correctly infers dynamically changing
13 activations of latent factors on synthetic dataset. Through fitting the infinite GPFA
14 model to population activities of hippocampal pyramidal cells during spatial naviga-
15 tion, we identify non-trivial and behavioural meaningful variability in neural
16 encoding process, and interpret neural variability from a novel perspective.

17 1 Introduction

18 Latent variable modelling is a popular class of unsupervised approaches for discovering low-
19 dimensional manifolds underlying high-dimensional neural population activities [Churchland et al.,
20 2007, Cunningham and Yu, 2014, Pei et al., 2021]. Accurate inference over the dynamical latent
21 processes allows us to perform exploratory analysis for identifying relevant behavioural correlates
22 of target neuron ensembles. However, a key limitation for such modelling is the necessity for pre-
23 specifying latent dimensions. This is usually performed based on model-selection approaches, such
24 as cross-validation and various information measures [Doya, 2007]. In the absence of prior knowl-
25 edge of encoded behavioural covariates underlying target neurons, heuristically selecting the latent
26 manifold dimensions lacks interpretability, and the selection is often sensitive with respect to model
27 hyperparameters and sampling process, hence leading to inconsistent inference outcomes. Alternative
28 approaches based on regularisation methods, such as automatic relevance determination [ARD; Wipf
29 and Nagarajan, 2007, Jensen et al., 2021], requires maximum likelihood (ML) learning based on
30 marginalisation over all training samples. Therefore, selection of the set of latent factors that are
31 mostly likely accounting for *all* observations, but not for *each* observation.

32 Here we propose a novel, probabilistically principled model that enables simultaneous posterior
33 inference of the number of latent factors and the set of activated latent factors pertinent to each
34 observation. Specifically, we develop a fully Bayesian nonparametric extension of the Gaussian
35 Process Factor Analysis (GPFA) model [Yu et al., 2008], a popular latent variable model for extracting
36 latent Gaussian process factors underlying population activities over single trials. The resulting model,

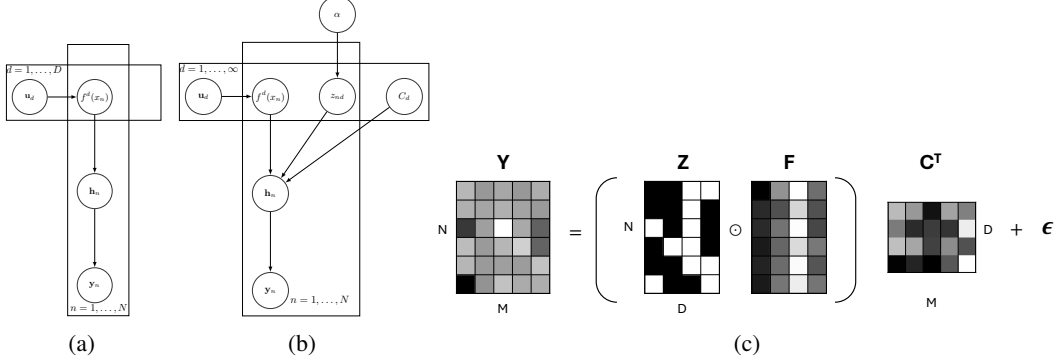


Figure 1: **Graphical demonstration of generative processes of GPFA and IBP models.** Generative models for standard (a) and infinite (b) GPFA models with sparse variational approximation. (c) Graphical illustration of IBP prior, in the form of weighted factor analysis model, with binary activations. Each observation \mathbf{y}_n is generated as a weighted sum of different set of latent factors with some additive noise. By taking the limit $D \rightarrow \infty$, we essentially place an IBP prior on the binary latent activation, \mathbf{Z} .

37 infinite GPFA, incorporates stochastic activation of latent factors in the loading process, which is
 38 modelled by the Indian Buffet Process (IBP) prior [Ghahramani and Griffiths, 2005]. The IBP defines
 39 a distribution over binary matrices with finite number of rows and infinite number of columns, hence
 40 enabling inference over the potentially infinite number of features, as well as tracking uncertainty
 41 associated with factor activations for each observation. Importantly, the latter feature allows us to
 42 investigate the nature of neural variability from a novel perspective: the variability in the expression of
 43 latent factors, potentially due to changes in internal states of the animal [Kelemen and Fenton, 2010,
 44 Flavell et al., 2022]. Through empirical evaluations on synthetic datasets, we show that the infinite
 45 GPFA model yields similar performance as standard GPFA model on dataset with constant generative
 46 process, but significantly outperforms GPFA when variability is introduced to the generative process.
 47 We further apply our model to population activities of hippocampal place cells recorded during
 48 spatial navigation tasks, and identify non-trivial variability in the neural encoding process, which is
 49 additionally contingent on the engaged task context.

50 2 Background

51 2.1 Gaussian Process Factor Analysis

52 GPFA extends standard factor analysis models, by replacing Gaussian factors with Gaussian Process
 53 factors for capturing non-trivial temporal dependencies over the latent space [Yu et al., 2008]. Similar
 54 to standard factor analysis model, GPFA assumes conditional independence between observation
 55 dimensions, given the latents. The generative model of GPFA is defined as following (Figure 1a).

$$\begin{aligned}
 \mathbf{f}_d(\cdot) &\sim \mathcal{GP}(m^d(\cdot), k^d(\cdot, \cdot)), & \text{for } d = 1, \dots, D, \\
 \mathbf{h}(x_n) &= \mathbf{C} \cdot \mathbf{F}(x_n) + \mathbf{d}, & \text{for } n = 1, \dots, N, \\
 \mathbf{y}(x_n) &\sim p(\mathbf{y}(x_n) | \phi(\mathbf{h}(x_n)), \theta), & \text{for } n = 1, \dots, N,
 \end{aligned} \tag{1}$$

56 where $m^d(\cdot)$ and $k^d(\cdot, \cdot)$ are the mean and kernel functions for the d -th latent factors, respectively¹,
 57 $\mathbf{C} \in \mathbb{R}^{M \times D}$ is the loading matrix that projects the latent factors to the neural space, with M being the
 58 number of neurons, \mathbf{d} is the offset for the linear transformation, $\mathbf{F}(x_n) = [\mathbf{f}_1(x_n) \ \dots \ \mathbf{f}_D(x_n)]$ is
 59 the column-stack of all latent factors at input location x_n , $\phi(\cdot)$ is some (non-linear) link function,
 60 and θ is some auxiliary generative parameters. Learning and inference with GPFA model can be
 61 performed using variational expectation-maximisation (EM), which we briefly review in the appendix.

¹We assume $m^d(\cdot) = 0$ unless stated otherwise.

62 **2.2 Indian Buffet Process**

63 The IBP defines a distribution over binary matrices with finite number of rows (observations) and
 64 infinite number of columns (latent factors) [Ghahramani and Griffiths, 2005]. Hence, by factorising
 65 the loading process in a factor analysis model into independent binary activation matrix, \mathbf{Z} , and
 66 activation weight matrix, \mathbf{C} , we can place an IBP prior over \mathbf{Z} for allowing stochastic loading of
 67 latent factors into each observation. Moreover, posterior inference over \mathbf{Z} allows for determination of
 68 the optimal set of latent factors pertinent to each observation, in a probabilistically principled manner.
 69 For interpretation, we consider the following Gaussian factor analysis model with stochastic latent
 70 activations (Figure 1c).

$$\begin{aligned}
 f_d &\sim \mathcal{N}(0, \sigma_d^2), \mathbf{C}_d \sim \mathcal{N}(\mathbf{0}, \nu_d^2 \mathbf{1}), & \text{for } d = 1, \dots, \infty, \\
 \pi_d &\sim \text{Beta}\left(\frac{\alpha}{D}, 1\right), & \text{for } d = 1, \dots, D, \\
 p(\mathbf{Z}|\boldsymbol{\pi}) &= \prod_{d=1}^D \pi_d^{m_d} (1 - \pi_d)^{N - m_d}, & (2) \\
 \mathbf{y}_n &= \mathbf{C}(\mathbf{Z}_n \odot \mathbf{F}) + \boldsymbol{\epsilon}_n, & \text{for } n = 1, \dots, N.
 \end{aligned}$$

71 We observe that $p(\mathbf{Z})$ models the probability for the n -th observation possessing the k -th factor, for
 72 all n and k . Taking the limit $D \rightarrow \infty$, it can be shown that the marginal distribution over \mathbf{Z} following
 73 the IBP distribution, and α controls the expected total number of latent factors (see details in the
 74 appendix). Posterior inference over the IBP-distributed \mathbf{Z} is intractable, but it is possible to perform
 75 approximate inference leveraging either MCMC or variational methods [Ghahramani and Griffiths,
 76 2005, Doshi et al., 2009]. Here we use the mean-field variational inference approach, which we
 77 briefly review in the appendix Doshi et al. [2009].

78 **3 Infinite GPFA**

79 Under the similar motivation behind the original proposal of IBP, we now propose infinite GPFA, the
 80 fully Bayesian nonparametric extension of standard GPFA that allows simultaneous inference over
 81 the optimal number of latent features and the set of most likely active latent factors underlying *each*
 82 observation. Specifically, the generative process of infinite GPFA is as following (Figure 1b).

$$\begin{aligned}
 \mathbf{f}_d(\cdot) &\sim \mathcal{GP}(0, k^d(\cdot, \cdot)), \quad \pi_d \sim \text{Beta}\left(\frac{\alpha}{D}, 1\right), \quad z_{nd}|\pi_d \sim \text{Bernoulli}(\pi_d), \\
 \mathbf{C}_d &\sim \mathcal{N}(\mathbf{0}, \nu_d^2 \mathbf{1}), \quad \mathbf{h}(x_n) = \mathbf{C} \cdot (\mathbf{Z} \odot \mathbf{F}(x_n)) + \mathbf{d}, \quad \mathbf{y}(x_n) \sim p(\mathbf{y}(x_n)|\phi(\mathbf{h}(x_n))), \quad \forall n, d,
 \end{aligned} \tag{3}$$

83 Here we use the finite Beta-Bernoulli approximation of the IBP distribution (Equation 2; [Ghahramani
 84 and Griffiths, 2005]). For the simplicity of demonstration, we assume both the loading weight matrix,
 85 \mathbf{C} , and concentration parameter, α , to be deterministic (but setting priors over \mathbf{C} and α is also
 86 possible, see Section 4.1 and appendix for further details). Note that the major difference between
 87 the generative processes of standard and infinite GPFA lies in their implementation of factor loading
 88 process, where standard GPFA assumes each latent GP factor is deterministically loaded into the
 89 observations, and infinite GPFA allows stochastic binary expression of latent factors that varies across
 90 each timestep and observation. Both learning of generative parameters and approximate inference
 91 over latent variables (\mathbf{f} , $\boldsymbol{\pi}$ and \mathbf{Z}) in the infinite GPFA model is achieved through variational learning,
 92 leveraging mean-field variational approximations. We further develop a sparse-variational extension
 93 of the infinite GPFA (infinite svGPFA), which greatly improves scalability. Further mathematical
 94 details of model learning and inference can be found in the appendix due to space constraints.

95 **4 Results**

96 **4.1 Empirical Evaluation on Synthetic Data**

97 We first consider synthetic population spikings generated from two sinusoidal latent processes,
 98 following the generic GPFA generative process with exponential link function and Poisson conditional
 99 likelihood (Equation 1). To demonstrate variations in neural encoding within a single trial, we

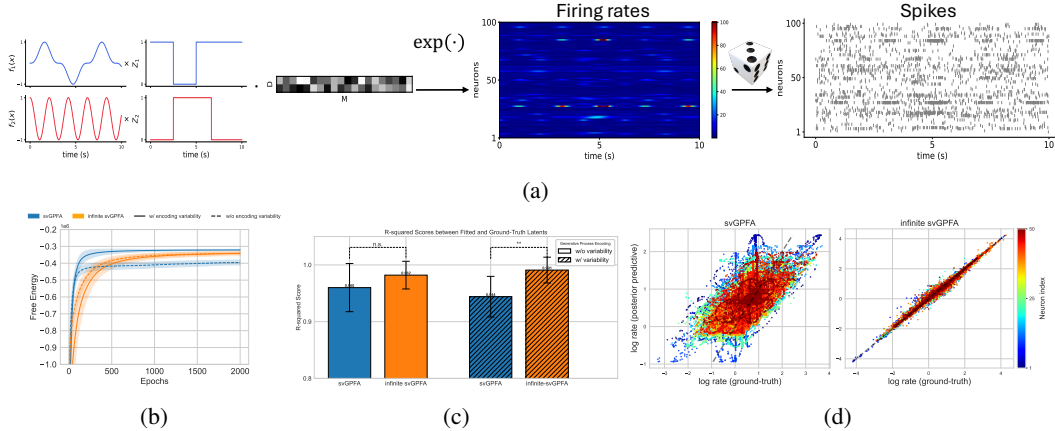


Figure 2: **Empirical evaluation of infinite svGPFA on synthetic dataset.** (a) Generative process for synthetic data, following the standard GPFA generative model with sinusoidal latent processes ($f_1(x) = \cos^3(x)$ and $f_2(x) = \sin(3x)$) and (optional) binary masking. The latents are linearly projected to the neural space, and passed through an exponential link function to generate firing rates, which are then used to generate spikes following time-inhomogeneous Poisson process. The binary masking, Z , represents within-trial variability in expression of latent factors in the neural activities. (b) Variational free energy objective during training for different models. (c) R-squared score between posterior means over latent processes and ground-truth latents, for svGPFA (blue) and infinite svGPFA (orange), on data given both generative processes (with and without encoding variability). (d) Log-log plot between logarithm of predicted and ground-truth firing rates for svGPFA (left) and infinite svGPFA (right). Different color represents different neurons. All evaluations are performed based on averaging over 10 random seeds where applicable.

optionally apply a multiplicative binary mask to the latent processes before projecting them to the neural space (Equation 3). We generate synthetic data for 100 neurons over 10 trials, each lasting 10 seconds in duration, for both cases with and without encoding variability (Figure 2a).

Under both generative processes, we fit standard and infinite svGPFA to corresponding population activities. We place Gaussian and Gamma priors over \mathbf{C} and α , respectively, hence additional marginalisation over them is required to compute the posterior distribution over latent processes (corresponding prior parameters are identical between svGPFA and infinite svGPFA where applicable). Both methods converge quickly under either data generative process (Figure 2b). Upon training completion², to validate the fidelity of fitted latents, we compare the R-squared score between the posterior means over the latent processes and the ground-truth latents for both models. For the baseline case with trivial binary masks, we observe that both models perform comparably well, reaching almost perfect discovery of latent processes driving the generation of neural activities. When encoding variability is introduced to binary masking, we observe that inferred latents of infinite svGPFA explains the ground-truth latents significantly better than those of standard svGPFA (one-sided student-t test, $p = 0.0028$). Such performance difference in model fitting is exacerbated through examining the accuracy of predicted firing rate: the svGPFA prediction is significantly noisier than the infinite svGPFA prediction, and the mean squared error of predicted log-rates is 0.40 ± 0.87 , which is again significantly higher than infinite svGPFA (0.0043 ± 0.025). Absence of explicit mechanisms accounting for variability in factor loading process in standard GPFA leads to greater deficits in learning the correct generative process. This is due to increased prediction errors in spiking observations induced by periods when at least one of the factors is not activated, which leads to learning of the wrong generative parameters to account for the gap.

4.2 Variability in Neural Encoding in Multi-Phase Spatial Navigation Tasks

We now probe the existence of variability in neural encoding and potential behavioural implications in real neural recordings. We apply our model to simultaneously recorded population activities of 204 pyramidal cells recorded from rat dorsal hippocampal CA1, whilst the rat is performing a spatial memory task [Pfeiffer and Foster, 2013]. Within each trial, given 36 uniformly arranged feeding

²All hyperparameters used in training can be found in Appendix

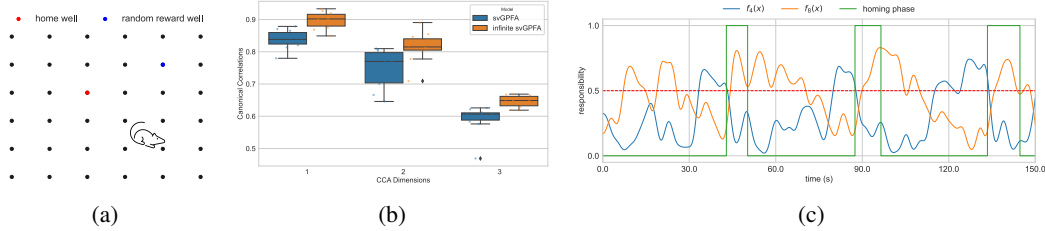


Figure 3: **Probing within-trial encoding variability in place cell population activities during spatial navigation with alternating behavioural phases.** (a) Illustration of behavioural task [Pfeiffer and Foster, 2013]. Rats navigate in a $2m \times 2m$ box, with 36 feeding wells uniformly arranged in the box. Animals alternate between searching for reward in a random well (*foraging* phase), and navigate back to a home well (*homing* phase). (b) We perform CCA between posterior mean over latent processes and selected behavioural variables for both infinite svGPFA and standard svGPFA. We show comparison of first three canonical correlations for the two models (dots represent different random seeds). (c) Temporal trace of posterior responsibilities associated with selected latent processes, and binary behavioural phase (green line, 0 and 1 indicate foraging and homing phases, respectively).

127 wells within a $2m \times 2m$ open-field arena (Figure 3a), rats learn to alternate between foraging for food
 128 in an unknown and random location (*foraging* phase), and returning to a fixed home location (*homing*
 129 phase). The transition to the next phase or trial is automatic upon consumption of the reward. We fit
 130 both standard and infinite svGPFA, with 10-dimensional latents to one recording session lasting 2187
 131 seconds, binning spike trains into spike counts within each 30 ms time window.

132 We perform canonical correlation analysis (CCA) between posterior mean of latent factors and relevant
 133 behavioural variables, including the 2-dimensional allocentric location, speed, and head direction of
 134 the animal [Hardoon et al., 2004, O’keefe and Nadel, 1978, Geisler et al., 2007]. Conforming with
 135 our findings from the synthetic experiment, we found that inferred latents from the infinite svGPFA
 136 model comprise more faithful representations of behavioural covariates than those from the standard
 137 svGPFA, indicated by the higher canonical correlations over all three principal directions.

138 We examine the activation of each latent factors across all timesteps. We observe high variability
 139 over time in posterior responsibilities for each latent (Figure 3c). Hence, despite stationarity in the
 140 marginal distribution of behavioural variables, the infinite svGPFA model predicts that the expression
 141 of these variables in population neural activities is not deterministic over time. By separating the
 142 continuous recording into alternating homing and foraging phases, we identify latent processes
 143 exhibiting selective activations in accordance with different behavioural phases. Specifically, we
 144 observe one latent process, $f_4(x)$, is usually increasingly activated during foraging phases and
 145 deactivated during homing phases (Figure 3c). From standard correlational analysis, we found that
 146 $f_4(x)$ is most strongly correlated with the speed of the animal. We identify another latent process,
 147 $f_8(x)$, being most strongly correlated with spatial location of the animal, which is activated at the
 148 beginning of homing phases, and decreasingly activated over the foraging phase. These comprise a
 149 coherent interpretation: speed is more actively represented during random foraging, potentially due
 150 to the importance of speed information in path integration (especially given extended trajectories),
 151 whereas during homing phases, the rat is usually running in straight trajectories back to the home
 152 location, potentially leveraging a pre-fixed strategy, hence leading to decreased representation of
 153 speed information, but increased representation of allocentric spatial location, in population activities.
 154 Collectively, we identify non-trivial temporal variability in encoding of behavioural correlates in
 155 population neural activities, and show that such variability is mediated by behavioural state of the
 156 animal through empirical verification.

157 5 Discussion

158 We introduce the infinite GPFA, a fully Bayesian nonparametric generalisation of standard GPFA
 159 models. The incorporation of the IBP prior over latent activations enables simultaneous inference over
 160 both the number of latent factors, as well as the most likely active set of latent factors underlying each
 161 observation. Through extensive evaluations on both synthetic and real neural datasets, we demonstrate
 162 improved empirical performance comparing to standard GPFA models. More importantly, we show
 163 that the infinite GPFA model is suited for exploring a gap in interpreting neural variability: the
 164 variability in neural encoding arising from changes in internal states of the animal.

165 **References**

- 166 Mark M Churchland, M Yu Byron, Maneesh Sahani, and Krishna V Shenoy. Techniques for extracting
167 single-trial activity patterns from large-scale neural recordings. *Current opinion in neurobiology*,
168 17(5):609–618, 2007.
- 169 John P Cunningham and Byron M Yu. Dimensionality reduction for large-scale neural recordings.
170 *Nature neuroscience*, 17(11):1500–1509, 2014.
- 171 Felix Pei, Joel Ye, David Zoltowski, Anqi Wu, Raeed H Chowdhury, Hansem Sohn, Joseph E
172 O’Doherty, Krishna V Shenoy, Matthew T Kaufman, Mark Churchland, et al. Neural latents
173 benchmark’21: evaluating latent variable models of neural population activity. *arXiv preprint*
174 *arXiv:2109.04463*, 2021.
- 175 Kenji Doya. *Bayesian brain: Probabilistic approaches to neural coding*. MIT press, 2007.
- 176 David Wipf and Srikantan Nagarajan. A new view of automatic relevance determination. *Advances*
177 *in neural information processing systems*, 20, 2007.
- 178 Kristopher Jensen, Ta-Chu Kao, Jasmine Stone, and Guillaume Hennequin. Scalable bayesian gpfa
179 with automatic relevance determination and discrete noise models. *Advances in Neural Information*
180 *Processing Systems*, 34:10613–10626, 2021.
- 181 Byron M Yu, John P Cunningham, Gopal Santhanam, Stephen Ryu, Krishna V Shenoy, and Maneesh
182 Sahani. Gaussian-process factor analysis for low-dimensional single-trial analysis of neural
183 population activity. *Advances in neural information processing systems*, 21, 2008.
- 184 Zoubin Ghahramani and Thomas Griffiths. Infinite latent feature models and the indian buffet process.
185 *Advances in neural information processing systems*, 18, 2005.
- 186 Eduard Kelemen and André A Fenton. Dynamic grouping of hippocampal neural activity during
187 cognitive control of two spatial frames. *PLoS biology*, 8(6):e1000403, 2010.
- 188 Steven W Flavell, Nadine Gogolla, Matthew Lovett-Barron, and Moriel Zelikowsky. The emergence
189 and influence of internal states. *Neuron*, 110(16):2545–2570, 2022.
- 190 Finale Doshi, Kurt Miller, Jurgen Van Gael, and Yee Whye Teh. Variational inference for the indian
191 buffet process. In *Artificial Intelligence and Statistics*, pages 137–144. PMLR, 2009.
- 192 Brad E Pfeiffer and David J Foster. Hippocampal place-cell sequences depict future paths to
193 remembered goals. *Nature*, 497(7447):74–79, 2013.
- 194 David R Hardoon, Sandor Szedmak, and John Shawe-Taylor. Canonical correlation analysis: An
195 overview with application to learning methods. *Neural computation*, 16(12):2639–2664, 2004.
- 196 John O’keefe and Lynn Nadel. *The hippocampus as a cognitive map*. Oxford university press, 1978.
- 197 Caroline Geisler, David Robbe, Michaël Zugaro, Anton Sirota, and György Buzsáki. Hippocampal
198 place cell assemblies are speed-controlled oscillators. *Proceedings of the National Academy of*
199 *Sciences*, 104(19):8149–8154, 2007.
- 200 Michalis Titsias. Variational learning of inducing variables in sparse gaussian processes. In *Artificial*
201 *intelligence and statistics*, pages 567–574. PMLR, 2009.
- 202 Lea Duncker and Maneesh Sahani. Temporal alignment and latent gaussian process factor inference
203 in population spike trains. *Advances in neural information processing systems*, 31, 2018.
- 204 Stephen Keeley, David Zoltowski, Yiyi Yu, Spencer Smith, and Jonathan Pillow. Efficient non-
205 conjugate gaussian process factor models for spike count data using polynomial approximations.
206 In *International conference on machine learning*, pages 5177–5186. PMLR, 2020.
- 207 Yee Whye Teh, Dilan Grür, and Zoubin Ghahramani. Stick-breaking construction for the indian
208 buffet process. In *Artificial intelligence and statistics*, pages 556–563. PMLR, 2007.

- 209 Adam Paszke, Sam Gross, Francisco Massa, Adam Lerer, James Bradbury, Gregory Chanan, Trevor
210 Killeen, Zeming Lin, Natalia Gimelshein, Luca Antiga, et al. Pytorch: An imperative style,
211 high-performance deep learning library. *Advances in neural information processing systems*, 32,
212 2019.
- 213 Diederik P Kingma and Jimmy Ba. Adam: A method for stochastic optimization. *arXiv preprint*
214 *arXiv:1412.6980*, 2014.

215 **A Further Model Details**

216 **A.1 Variational Learning for GPFA**

217 We consider the standard GPFA generative process (Equation 1). We use variational expectation-
 218 maximisation (EM) methods for approximate inference over latent processes in GPFA. Specifically,
 219 we leverage the mean-field sparse-variational approximation based on inducing points for scalability
 220 purposes [Titsias, 2009], which renders desirable conditional independence in the variational free
 221 energy objective.

$$q(\mathbf{F}, \mathbf{U}) = \prod_{d=1}^D p(\mathbf{f}_d | \mathbf{u}_d) q(\mathbf{u}_d), \quad \mathcal{F}[q] = \sum_x \langle \log p(\mathbf{y} | \phi(\mathbf{h})) \rangle_{q(\mathbf{h})} - \sum_{d=1}^D \text{KL}[q(\mathbf{u}_d) || p(\mathbf{u}_d)], \quad (4)$$

222 where \mathbf{u}_d are the inducing points for the d -th latent factor.

223 From standard Gaussian identity, we know that the conditional likelihood $p(\mathbf{f}_d(\mathbf{x}) | \mathbf{u}_d)$ is also Gaussian,
 224 with mean $\mathbf{K}_{\mathbf{xw}}^d (\mathbf{K}_{\mathbf{ww}}^d)^{-1} \mathbf{u}_d$ and covariance $\mathbf{K}_{\mathbf{xx}}^d - \mathbf{K}_{\mathbf{xw}}^d (\mathbf{K}_{\mathbf{ww}}^d)^{-1} (\mathbf{K}_{\mathbf{xw}}^d)^T$, where $\mathbf{K}_{\mathbf{xw}}^d \in \mathbb{R}^{N \times S}$ such
 225 that $(\mathbf{K}_{\mathbf{xw}}^d)_{nd} = k^d(x_n w_d)$. Hence, given $q(\mathbf{u}_d) = \mathcal{N}(\boldsymbol{\mu}_d^u, \mathbf{S}_d^u)$, we could easily compute the
 226 marginal variational approximation for \mathbf{f} , $q(\mathbf{f}_d) = \mathcal{N}(\boldsymbol{\mu}_d^f, \mathbf{S}_d^f)$.

$$\boldsymbol{\mu}_{nd}^f = k^d(x_n, \mathbf{w}) (\mathbf{K}_{\mathbf{ww}}^d)^{-1} \boldsymbol{\mu}_d^f, \quad (s_{nd}^f)^2 = k_{nn}^d + k_{n\mathbf{w}}^d ((\mathbf{K}_{\mathbf{ww}}^d)^{-1} \mathbf{S}_d^u (\mathbf{K}_{\mathbf{ww}}^d)^{-1} - (\mathbf{K}_{\mathbf{ww}}^d)^{-1}) k_{\mathbf{wn}}^d, \quad (5)$$

227 Note that $q(\mathbf{h})$ is additively GP-distributed (Equation 1). In general, the expected log conditional
 228 likelihood can only be evaluated approximately [Duncker and Sahani, 2018, Keeley et al., 2020].
 229 However, it is possible to compute the expected log conditional-likelihood under certain assumptions
 230 of conditional likelihood and link function (e.g., Gaussian observation and identity link function).
 231 The KL divergence between the variational approximation and GP prior over the inducing points can
 232 be evaluated analytically.

233 **A.2 Variational Inference for IBP**

234 We re-iterate the weighted factor analysis generative process below.

$$\begin{aligned} f_d &\sim \mathcal{N}(0, \sigma_d^2), \quad \mathbf{C}_d \sim \mathcal{N}(\mathbf{0}, \nu_d^2 \mathbf{1}), & \text{for } d = 1, \dots, \infty, \\ \pi_d &\sim \text{Beta}\left(\frac{\alpha}{D}, 1\right), & \text{for } d = 1, \dots, D, \\ p(\mathbf{Z} | \boldsymbol{\pi}) &= \prod_{d=1}^D \pi_d^{m_d} (1 - \pi_d)^{N - m_d}, & (6) \\ \mathbf{y}_n &= \mathbf{C}(\mathbf{Z}_n \odot \mathbf{F}) + \boldsymbol{\epsilon}_n, & \text{for } n = 1, \dots, N. \end{aligned}$$

235 Given the conjugacy between Beta and binomial distributions, we can analytically marginalise $\boldsymbol{\pi}$ out.

$$p(\mathbf{Z}) = \prod_{d=1}^D \frac{\frac{\alpha}{D} \Gamma(m_d + \frac{\alpha}{D}) \Gamma(N - m_d + 1)}{\Gamma(N + 1 + \frac{\alpha}{D})}, \quad (7)$$

236 Taking the limit $D \rightarrow \infty$, the IBP places a prior on $[\mathbf{Z}]$, the canonical form of \mathbf{Z} that is permutation-
 237 invariant [Ghahramani and Griffiths, 2005].

$$p([\mathbf{Z}]) = \frac{\alpha^{\mathfrak{D}} \exp(-\alpha H_N)}{\prod_{h \in \{0,1\}^N \setminus \mathbf{0}} \mathfrak{D}_h!} \prod_{d=1}^{\mathfrak{D}} \frac{(N - m_d)! (m_d - 1)!}{N!} \quad (8)$$

238 where \mathfrak{D} is the number of non-zero columns in \mathbf{Z} , $H_N = \sum_{n=1}^N \frac{1}{n}$ is the N -th harmonic number, m_d
 239 is the number of one-entries in the d -th column of \mathbf{Z} , \mathfrak{D}_h is the number of occurrences of non-zero
 240 binary column vector h in \mathbf{Z} , α is the prior parameter that controls the expected number of features
 241 present in each observation.

242 A useful interpretation of IBP is based on the stick-breaking formulation [Teh et al., 2007], which
 243 interprets π_d being constructed by stick-breaking weights, $\pi_d = \prod_{i=1}^d v_d$, where $v_d \sim \text{Beta}(\alpha, 1)$.
 244 We hence see that the probability of employing the d -th latent factor decreases exponentially with d ,
 245 and α controls the expected number of latents.

246 Inference given the IBP prior can be performed with either MCMC or variational methods [Ghahra-
 247 mani and Griffiths, 2005, Doshi et al., 2009]. Here we briefly review the finite mean-field variational
 248 inference approach outlined in Doshi et al. [2009].

$$\begin{aligned} q(\pi_d|a_d, b_d) &= \text{Beta}(a_d, b_d), \quad \forall d, \\ q(\mathbf{C}_d|\boldsymbol{\mu}_d, \mathbf{S}_d) &= \mathcal{N}(\boldsymbol{\mu}_d, \mathbf{S}_d), \quad \forall d, \\ q(z_{nd}|\tau_{nd}) &= \text{Bernoulli}(\tau_{nd}), \quad \forall n, d, \end{aligned} \quad (9)$$

249 Given the conditional independence within the generative model, the variational free energy objective
 250 takes the following expression³.

$$\begin{aligned} \mathcal{F}[q] &= \langle \log p(\boldsymbol{\pi}, \mathbf{C}, \mathbf{Z}, \mathbf{Y}) - \log q(\boldsymbol{\pi})q(\mathbf{C})q(\mathbf{Z}) \rangle \\ &= \sum_{d=1}^D \langle \log p(\pi_d) \rangle + \sum_{d=1}^D \langle \log p(\mathbf{C}_d) \rangle + \sum_{n=1}^N \sum_{d=1}^D \langle \log p(z_{nd}|\pi_d) \rangle + \sum_{n=1}^N \langle \log p(\mathbf{y}_n|\mathbf{Z}_n, \mathbf{C}) \rangle + \mathbb{H}[q] \end{aligned} \quad (10)$$

251 A.3 Variational Learning for Infinite GPFA

252 We perform variational learning using the finite mean-field variational approximations, $q(\mathbf{U}, \boldsymbol{\pi}, \mathbf{Z}) =$
 253 $\prod_{d=1}^D [q(\mathbf{u}_d)q(\pi_d) \prod_n p(z_{nd})]$.

$$\begin{aligned} q(\mathbf{u}_d|\boldsymbol{\mu}_d^u, \mathbf{S}_d^u) &= \mathcal{N}(\mathbf{u}_d|\boldsymbol{\mu}_d^u, \mathbf{S}_d^u), \quad \forall d, \\ q(\pi_d|a_d, b_d) &= \text{Beta}(\pi_d|a_d, b_d), \quad \forall d, \\ q(z_{nd}|\tau_{nd}) &= \text{Bernoulli}(\tau_{nd}), \quad \forall n, d, \end{aligned} \quad (11)$$

254 Note that in the above formulation, by default we have assumed sparse variational approximation
 255 treatment for scalability purposes.

256 Given the conditional independence in the generative process, we could express the variational free
 257 energy as following.

$$\begin{aligned} \mathcal{F}[q] &= \langle \log p(\mathbf{Y}, \mathbf{F}, \boldsymbol{\pi}, \mathbf{Z}) - \log q(\mathbf{F}, \boldsymbol{\pi}, \mathbf{Z}) \rangle \\ &= \sum_{n=1}^N \langle \log p(\mathbf{y}_n|\mathbf{F}_n, \mathbf{Z}_n) \rangle - \sum_{d=1}^D \text{KL}[q(\mathbf{u}_d)||p(\mathbf{u}_d)] - \sum_{d=1}^D \text{KL}[q(\pi_d)||p(\pi_d)] - \sum_{n,d} \langle \text{KL}[q(z_{nd})||p(z_{nd})] \rangle_{q(\pi_d)} \end{aligned} \quad (12)$$

258 Given the variational distributions, all terms always admit analytical expression apart from expected
 259 conditional log-likelihoods. Due to the non-Gaussian nature of $q(\mathbf{h})$, previous approximation ap-
 260 proaches based on Gaussian quadrature no longer applies [Duncker and Sahani, 2018]. Instead, we
 261 leverage second-order Taylor expansion for approximating the expected conditional log-likelihood,
 262 which offers an effective tradeoff between computational efficiency and approximation accuracy
 263 (see Supplemental Section 2 for details). However, we note that under the special case of Gaus-
 264 sian conditional likelihood with identity link function, it is possible to evaluate such expectation
 265 analytically.

$$\langle \log p(\mathbf{y}_n|\mathbf{F}_n, \mathbf{Z}_n) \rangle = -\frac{1}{2\sigma^2} \sum_{m=1}^M \langle (y_{nm} - h_{nm})^2 \rangle = -\frac{1}{2\sigma^2} \sum_{m=1}^M ((y_{nm} - \langle h_{nm} \rangle)^2 + \text{Var}[h_{nm}]), \quad (13)$$

³Unless necessary, we do not explicitly show the variational distributions the expectation is taken with respect to for notational simplicity.

266 Given the mean-field assumption, we could analytically evaluate the expectation and variance of h_{nm}
 267 with respect to the variational distributions.

$$\begin{aligned} \langle h_{nm} \rangle &= \mathbf{C}_m \cdot (\boldsymbol{\tau}_n \odot \boldsymbol{\mu}_n^f) + d_m, \\ \text{Var}[h_{nm}] &= \mathbf{C}_m^{\odot 2} \cdot \left(\boldsymbol{\tau}_n^2 \odot (\mathbf{s}_n^f)^2 + ((\boldsymbol{\mu}_n^f)^{\odot 2} + (\mathbf{s}_n^f)^{\odot 2}) \odot \boldsymbol{\tau}_n \odot (1 - \boldsymbol{\tau}_n) \right) \end{aligned} \quad (14)$$

268 where $\boldsymbol{\mu}_n^f$ and $(\mathbf{s}_n^f)^2$ are the mean and diagonal-variance of $\mathbf{F}(x_n)$, respectively, and \odot^2 repre-
 269 sents the elementwise square operation. We have leveraged the law of total variance, $\text{Var}[XY] =$
 270 $\mathbb{E}[\text{Var}[XY]] + \text{Var}[\mathbb{E}[XY]]$. The complete derivation of variational free energy for the finite varia-
 271 tional approach can be found in Supplemental Section 2.

272 The model is learned via variational EM, iteratively updating the variational parameters (Equation 11),
 273 and the generative model parameters (i.e., \mathbf{C} , \mathbf{d} and α), via gradient-based updates that maximises the
 274 free energy objective. In practice, we employ standard automatic differentiation framework for such
 275 gradient-based learning [Paszke et al., 2019].

276 B Experiment Details

277 All models are trained with Adam optimiser [Kingma and Ba, 2014], with learning rate 0.01. For the
 278 main experimental evaluations, we train all models over 2000 epochs. All evaluations are based on
 279 averaging over 10 random seeds where applicable.

280 **Synthetic Data.** We instantiate both the standard GPFA and infinite GPFA models with stochastic \mathbf{C} ,
 281 where $\nu_d^2 = 0.1$. We set the number of inducing points to be 30 for the main evaluations, and the
 282 corresponding inducing locations are randomly initialised and trained. For all models, we use the
 283 squared exponential (SE) kernels, with trainable scale and lengthscale parameters.

$$k^d(x, x') = s_d^2 \exp\left(-\frac{\|x - x'\|}{\tau_d^2}\right), \quad (15)$$

284 **Neural Data.** We preprocess the spiking train data into spike counts, with $30ms$ time window. The
 285 instantaneous firing rates for each neuron are computed via dividing the spike counts by the time
 286 window size, followed by Gaussian smoothing. The loading matrix, \mathbf{C} , is assumed to be deterministic,
 287 hence is learned through the variational M-step. The concentration parameters, α , is again assumed
 288 to be stochastic, with Gamma prior and parameters $s_1 = 1.0$, $s_2 = 1.0$. For all models, the number
 289 of inducing points are 100, and corresponding inducing locations are fixed as equally spaced location
 290 along the input (time) domain. We again use the SE kernels for the latent GPs with trainable scale
 291 and lengthscale parameters.

292 For segmenting the continuous recordings into separate foraging and homing phases, we note that
 293 animals often lowers their speed upon consuming the food, and we can use this feature as a marker
 294 for the segmentation. Hence, we identify all periods with low speed ($< 1cm/s$) and within proximity
 295 of the reward location ($< 5cm$) as the end of the homing phase, and all other periods with speed
 296 ($< 1cm/s$) over an extended time span ($> 10s$) as the end of the foraging phase.